

An excess of damped Lyman α galaxies near QSOs.

David M. Russell^{1,2*} Sara L. Ellison³ and Chris R. Benn¹

¹*Isaac Newton Group, Apartado 321, E-38700 Santa Cruz de La Palma, Spain*

²*School of Physics & Astronomy, University of Southampton, Highfield, Southampton, SO17 1BJ, United Kingdom*

³*Dept. Physics & Astronomy, University of Victoria, 3800 Finnerty Rd, Victoria, BC, V8P 1A1, Canada*

29 April 2021

ABSTRACT

We present a sample of 33 damped Lyman alpha systems (DLAs) discovered in the Sloan Digital Sky Survey (SDSS) whose absorption redshifts (z_{abs}) are within 6000 km s⁻¹ of the QSO's systemic redshift (z_{sys}). Our sample is based on 731 $2.5 < z_{\text{sys}} < 4.5$ non-broad-absorption-line (non-BAL) QSOs from Data Release 3 (DR3) of the SDSS. We estimate that our search is $\approx 100\%$ complete for absorbers with $N(\text{H I}) \geq 2 \times 10^{20}$ cm⁻². The derived number density of DLAs per unit redshift, $n(z)$, within $\Delta v < 6000$ km s⁻¹ is higher (3.5σ significance) by almost a factor of 2 than that of intervening absorbers observed in the SDSS DR3, i.e. there is evidence for an overdensity of galaxies near the QSOs. This provides a physical motivation for excluding DLAs at small velocity separations in surveys of intervening ‘field’ DLAs. In addition, we find that the overdensity of proximate DLAs is independent of the radio-loudness of the QSO, consistent with the environments of radio-loud and radio-quiet QSOs being similar.

Key words: quasars: general - quasars: emission lines - radio continuum: galaxies - early Universe

1 INTRODUCTION

Ly α absorption lines in the spectra of high redshift QSOs trace the distribution of neutral hydrogen along the lines of sight to the background sources. Studying the properties of these intervening absorption systems can provide insights into a range of cosmic structures, ranging from the intergalactic medium to protogalaxies. The absorbers with the highest column densities give rise to lines with characteristic Lorentzian profiles. Specifically, damped Ly α (DLA) systems, defined as having $N(\text{H I}) \geq 2 \times 10^{20}$ cm⁻², dominate the mass density of HI in the universe and are believed to be associated with the progenitors of present day galaxies. Studies of DLAs have furnished a wealth of information about the density and chemical enrichment of galaxy-scale clouds of neutral hydrogen at early epochs (see for example the reviews by Pettini 2004; Wolfe, Gawiser & Prochaska 2005).

Nearly all existing studies of DLAs have been confined to absorbers lying beyond a certain velocity from the systemic redshift of the QSO (z_{sys}). The velocity cut imposed is somewhat subjective and survey dependent, but is usually 3000 – 6000 km s⁻¹ blueward of z_{sys} . The motivation for excluding proximate DLAs ($\Delta v < 6000$ km s⁻¹, PDLAs) is

two-fold. First, studies of the Ly α forest have revealed the existence of a ‘proximity effect’, whereby the high UV flux from the QSO causes additional ionisation of the diffuse HI clouds within a few Mpc of the QSO (e.g. Bajtlik, Duncan & Ostriker 1988; Lu, Wolfe & Turnshek 1991). Even high column density systems whose interstellar media (ISM) are usually considered to be self-shielded can be affected by proximity to a powerful ionising source such as a QSO. For example, it has been noted that PDLAs seem to preferentially exhibit Ly α emission superimposed on the Ly α absorption trough (e.g. Ellison et al. 2002 and references therein). More recently, Adelberger et al. (2005) have detected Ly α fluorescence in a DLA separated by 380 (proper) h_{70}^{-1} kpc from a $z = 2.84$ QSO. Excluding absorbers which may be affected by the QSO's ionising radiation simplifies the calculations of its total hydrogen content and chemical abundances. Second, studies concerned with the statistical properties of *intervening* galaxies could be affected by the inclusion of material associated with the QSO. Intrinsic absorption could, for example, be associated with BAL-like outflows or with the QSO host galaxy. However, the one $z_{\text{abs}} \sim z_{\text{sys}}$ PDLA with measured metal abundances is known to have a metallicity $\sim 15\%$ of the solar value (Meyer, Welty & York 1989; Lu et al. 1996). This value is typical of intervening DLAs but inconsistent with the typically solar or super-solar metallicities of BAL-like outflows and intrinsic systems (Barlow &

* Email: davidr@phys.soton.ac.uk

Sargent 1997; Petitjean, Rauch & Carswell 1994; D’Orolicio et al. 2004). The PDLAs also lack the strong CIV or NV absorption and complex absorption profiles characteristic of BALs (see also Møller, Warren & Fynbo 1998). Taken together, this evidence implies that PDLAs are more likely to be related to gas associated with galaxies rather than AGN. The differences in redshift between QSOs and PDLAs are typically too large for the absorbing material to be part of the QSO host galaxy suggesting that PDLAs may have an origin similar to the intervening systems, but are simply located closer to the QSO.

In this paper, we consider whether there may be further justification for excluding PDLAs from surveys by investigating whether they are drawn from the same ‘random’ population as the intervening absorbers. It has been known for more than 30 years that QSOs are often associated with galaxy evolution (e.g. Bahcall, Schmidt & Gunn 1969) so it is plausible that PDLAs may represent a subset of early galaxies in a distinct environment. For example, it is well-established that overdensities of galaxies are often seen in the vicinity of QSOs (e.g. Yee & Green 1987; Ellingson, Green & Yee 1991; Yamada et al. 1997; Hall & Green 1998; Hall, Green & Cohen 1998; Sanchez & Gonzalez-Serrano 1999; McLure & Dunlop 2001; Wold et al. 2001; Finn, Impey & Hooper 2001; Clements 2000; Sanchez & Gonzalez-Serrano 2002). Our objective is therefore to determine whether DLAs located at velocities $< 6000 \text{ km s}^{-1}$ from the background QSO may similarly inhabit distinct environments compared with intervening ‘field’ absorbers. As a first approach, we compare the number density of PDLAs to that of traditionally selected $z_{\text{abs}} \ll z_{\text{sys}}$ DLAs. A number density of PDLAs consistent with that of intervening DLAs would imply no distinction in their respective environments. Conversely, an excess of DLAs near the QSO’s systemic redshift could be interpreted as probing galaxy overdensities analogous to those found by imaging surveys. Overdensities of PDLAs would provide an empirically motivated cut-off for intervening DLA searches whose goal is to study an unbiased sample of absorbers.

Since the majority of DLA surveys exclude PDLAs, constructing a statistical sample from the literature is challenging. A handful of PDLAs have been reported (e.g. Møller & Warren 1993; Pettini et al. 1995; Møller et al. 1998; Ellison et al. 2002) but they have not been generally included in published lists of DLAs. Recently, Ellison et al. (2002) searched for PDLAs in the Complete Optical and Radio Absorption Line System (CORALS) sample (see Ellison et al. 2001 for full sample definition). Combining their sample with PDLAs discovered in previous surveys of radio loud and radio quiet QSOs (RLQs and RQQs respectively) Ellison et al. (2002) found 4 PDLAs within $\Delta v < 3000 \text{ km s}^{-1}$ of 96 radio-loud QSOs, and just 1 within $\Delta v < 3000 \text{ km s}^{-1}$ of 49 radio-quiet QSOs (Péroux et al. 2001). Given the redshift path (Δz) covered by the RQQ sample, the detection of one PDLA is consistent with the known number density per unit redshift ($n(z)$) of intervening absorbers. However, the detection of four PDLAs associated with RLQs implies that the number density of PDLAs is > 4 times that of the intervening population. This apparent overdensity around RLQs at $z > 2$ is significant only at the 1.5σ level due to the relatively small number of QSOs, and Ellison et al. (2002) noted that better statistics are required to confirm the overdensity.

Table 1. Metal-line rest-frame wavelengths

Line	Wavelength (Å)
O I	1302.17
Si IV	1393.76
Si IV	1402.77
Si II	1526.71
C IV	1548.20
C IV	1550.78
Fe II	1608.45
Al II	1670.79
Al III	1854.72

With the advent of the Sloan Digital Sky Survey (SDSS), the spectra of large numbers of QSOs ($\sim 10^5$, eventually) are becoming available. Here we search for PDLAs in the spectra of 731 QSOs with apparent magnitude $i \lesssim 20.5$ from the SDSS Data Release 3 (DR3, Abazajian et al. 2005), in order to answer the following two questions:

- Is the density of DLAs in the vicinity of QSOs significantly higher than that along the line of sight?
- Do the environments of radio-quiet and radio-loud QSOs differ?

This work improves on that of Ellison et al. (2002) in several ways. First, our sample is an order of magnitude larger than the CORALS survey. With these improved statistics we can investigate the number density in a range of velocity bins from z_{sys} . Since the data quality of the SDSS spectra is somewhat heterogeneous, we have carried out completeness tests for our sample; these are described in §3. Finally, we use a Monte Carlo simulation to assess the significance of the measured overdensity of PDLAs relative to intervening systems.

We have adopted the ‘consensus’ cosmology model with $H_0 = 70 \text{ km s}^{-1} \text{ Mpc}^{-1}$, $\Omega_\Lambda = 0.7$, $\Omega_M = 0.3$.

2 THE SAMPLE

SDSS DR3 covers $\sim 5300 \text{ deg}^2$, mainly in the northern sky, and includes spectra of 5×10^4 QSOs with $i \lesssim 20.5$. From these, we selected 1885 $2.5 < z_{\text{sys}} < 4.5$ QSOs. The lower redshift limit was selected so that at least 250 Å of the Ly α forest was covered by the SDSS spectrum (whose blue limit is $\approx 4000 \text{ Å}$). The upper redshift limit was imposed to avoid the difficulty of identifying DLAs unambiguously in the much noisier and densely populated Ly α absorption forests of QSOs at higher redshift. The 1885 spectra were inspected individually, and 413 objects showing broad absorption lines just blueward of the CIV emission line were rejected. These are probable broad-absorption-line (BAL) QSOs, and a search for proximate DLAs could be confused by HI absorption features associated with the BAL clouds¹. BAL QSOs were rejected on the basis of visual inspection,

¹ This selection left within the sample one object meeting the formal criteria for a BAL (0140–0839) but with the absorption detached $\sim 27000 \text{ km s}^{-1}$ blueward of the CIV emission, i.e. not contaminating the part of the spectrum searched for PDLAs.

Table 2. DLAs within 6000 km s^{-1} of the redshift of SDSS DR3 QSOs

RA J2000 (1)	Dec J2000 (2)	i (3)	z_{sys} (4)	S:N (5)	$S_{1.4\text{GHz}}$ mJy (and $\log_{10} R$) (6)	$N(\text{H I})$ 10^{20} cm^{-2} (7)	z_{abs} (8)	Δv km s^{-1} (9)	Metal lines (10)
01 40 49.18	-08 39 42.5	17.7	3.713	7.5	-	4.5	3.696	1085	OI SiII [BAL]
07 39 38.85	+30 59 51.2	20.4	3.399	9.2	6.69 (2.9)	2.0	3.353	3160	SiII CIV
08 05 53.02	+30 29 37.3	19.9	3.432	9.9	-	2.5	3.429	200	OI SiII CIV
08 11 14.32	+39 36 33.2	20.1	3.092	6.9	-	7.0	3.037	4060	
08 26 38.59	+51 52 33.2	17.2	2.850	5.9	-	5.5	2.833	1330	OI SiIV SiII CIV FeII AlII
08 44 51.72	+05 18 27.8	20.0	4.465	7.2	-	3.5	4.376	4925	
09 09 30.42	+07 00 50.7	20.3	3.273	5.5	-	3.0	3.219	3815	
09 40 35.93	+50 03 08.7	20.1	3.567	5.8	-	2.5	3.500	4435	
10 11 22.59	+47 00 42.2	19.0	2.928	9.1	29.56 (2.5)	2.5	2.909	1490	OI SiII
10 26 19.09	+61 36 28.9	18.6	3.849	5.3	-	3.0	3.785	3985	OI SiIV SiII CIV AlII
10 45 01.44	+50 40 45.9	20.0	3.998	5.1	-	6.0	3.949	2955	
10 48 20.93	+50 32 54.2	20.2	3.889	12.0	-	15.0	3.815	4545	OI SiIV CIV
11 12 24.18	+00 46 30.3	19.7	4.035	14.0	-	19.0	3.958	4620	OI AlII
11 26 48.62	+05 56 28.1	19.6	3.191	17.1	-	7.0	3.147	3165	
12 27 23.65	+01 48 06.0	20.4	2.881	10.1	-	2.0	2.876	425	
12 42 04.27	+62 57 12.1	19.6	3.321	5.7	0.88 (1.4)	2.0	3.276	3140	SiIV SiII CIV FeII AlII
12 48 30.64	+49 14 00.2	20.4	3.079	7.7	-	4.0	3.032	3460	
12 57 59.22	-01 11 30.2	18.7	4.112	8.1	-	2.0	4.022	5330	OI SiIV CIV
13 25 21.27	+52 45 13.1	19.8	3.953	6.3	-	2.5	3.861	5625	OI
13 41 00.13	+58 07 24.2	19.4	3.500	7.3	-	7.0	3.417	5585	all those listed in Table 1
13 46 37.94	+56 49 15.6	19.7	3.463	6.7	-	3.0	3.430	2225	OI
14 00 29.01	+41 12 43.4	19.0	2.540	5.9	-	45.0	2.537	255	OI SiII CIV FeII AlII
14 20 41.96	+42 22 57.0	19.6	3.378	8.2	-	2.0	3.336	2925	OI
14 51 20.65	+39 13 50.4	20.4	3.376	8.3	-	2.0	3.307	4770	SiII CIV
15 12 54.37	-00 56 36.6	20.2	4.457	5.6	-	8.0	4.400	3150	OI SiIV SiII CIV FeII
15 52 48.01	+56 03 28.9	20.0	3.604	12.4	-	2.0	3.556	3145	
16 08 13.86	+37 47 27.3	20.3	3.996	8.5	-	2.0	3.952	2655	OI SiIV
16 11 19.56	+44 11 44.0	20.0	4.024	5.1	-	5.0	3.982	2520	SiIV
17 04 21.85	+62 47 41.5	20.1	2.980	6.0	-	6.0	2.953	2040	OI SiIV
17 18 00.20	+62 13 25.6	19.8	3.670	7.8	-	3.5	3.618	3360	OI SiII FeII AlII
17 20 07.20	+60 28 23.8	20.4	4.425	8.6	5.06 (2.2)	5.0	4.326	5525	
21 00 25.03	-06 41 46.0	18.1	3.138	9.0	-	9.0	3.092	3350	all those listed in Table 1
21 22 07.36	-00 14 45.7	19.0	4.072	5.2	-	2.5	4.001	4230	OI CIV

The columns give: (1-4) SDSS RA, Dec, i mag and emission-line redshift; (5) S:N in the continuum redward of the Ly α emission; (6) FIRST 1.4-GHz radio flux density (and $\log_{10} R$ where R is the radio-loudness parameter (see §2); $\log_{10} R > 1.0$ for a RLQ); (7) fitted H I column density of the DLA; (8) DLA redshift; (9) DLA velocity, relative to z_{sys} ; (10) metal lines associated with the DLA

and all three authors independently checked the classifications.

We rejected 665 spectra with continuum signal-to-noise ratio per pixel (S:N) less than 5.0 in the continuum redward of the Ly α emission, based on the S:N estimates (in g , r and i bands) included in the headers of the SDSS spectra. We also measured the S:N directly from the spectrum in a

sample of 50 QSOs and found that 90% of our measured S:N agree with the quoted S:N within 0.2.

Finally, to ensure availability of radio flux densities (or limits) for the QSOs, we rejected the 76 QSOs not falling within areas covered by the FIRST survey (Faint Images of the Radio Sky at Twenty cm, $S_{1.4\text{GHz}} \gtrsim 1 \text{ mJy}$; Becker, White & Helfand 1995). This left a final sample of 731 QSOs

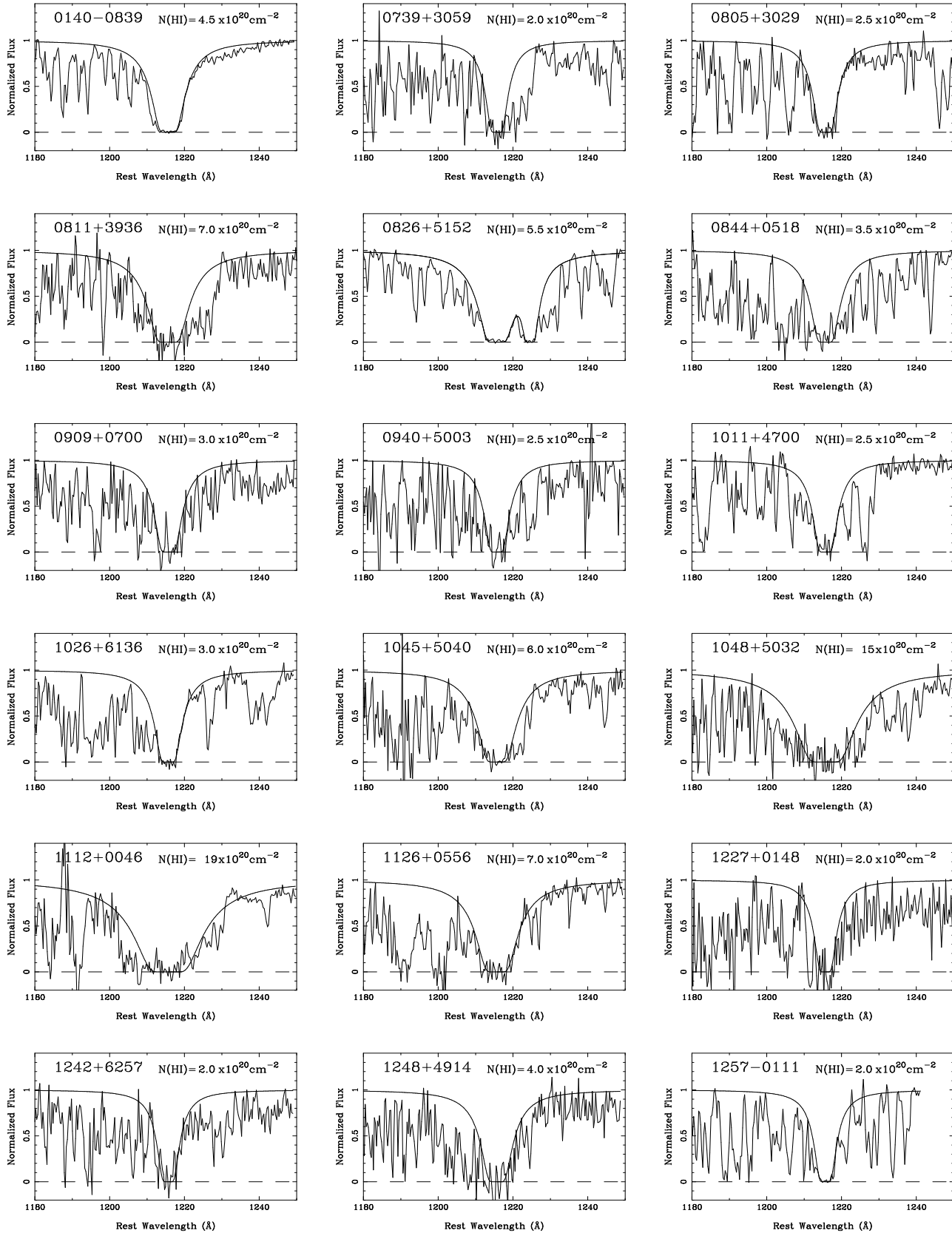


Figure 1. Theoretical damped Ly α profile fits to all 33 PDLAs. The fitted $N(\text{H I})$ is indicated at the top right of each plot. Table 2 gives the derived z_{abs} for each absorption system. For QSO 0826+5152, the fit is for the two absorbers, and the wavelength scale is in the rest frame of the blueward feature, which is the PDLA in this system. The HI column density of the redward absorber is $1.3 \times 10^{20} \text{ cm}^{-2}$.

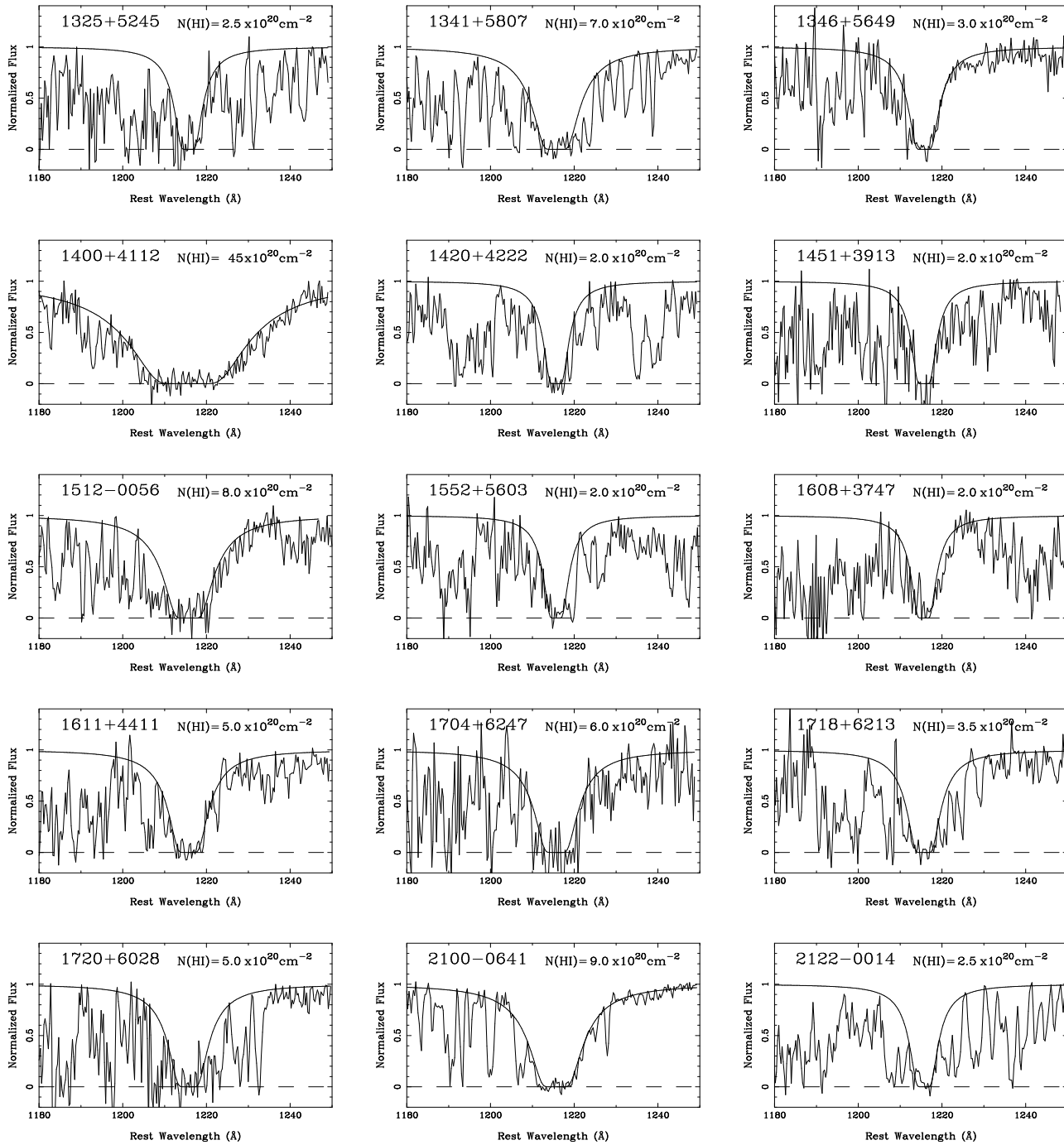


Figure 1 – continued

satisfying the following criteria: $2.5 < z_{\text{sys}} < 4.5$; $i \gtrsim 20.5$ (the SDSS limit); continuum S:N > 5.0 redward of the Ly α emission; non-BAL; and within the area covered by FIRST.

Radio counterparts were sought in the FIRST catalogue and sources within 2 arcsec of the optical position were assumed to be true radio identifications. The radio images of other sources lying within 30 arcsec of the QSO (9 in all) were inspected individually. None of these lie ≤ 5 arcsec from a line joining the two radio counterparts, and so the 9 are assumed to be unrelated sources. Based on the FIRST source density, we estimate the expected num-

ber of chance radio–optical coincidences to be 0.06. Following Stocke et al. (1992), we take as our definition of radio loud: $\log_{10} R > 1.0$, where R (radio-loudness parameter) is the ratio of K-corrected radio and optical flux densities: $F_{\nu}(5\text{GHz})/F_{\nu}(2500\text{\AA})$. The 5-GHz radio flux density was obtained from the FIRST 1.4-GHz flux density, assuming a mean radio spectral index $\alpha = -0.3$ ($S_{\nu} \propto \nu^{\alpha}$). Of the 731 QSOs in the sample, 94 are radio-loud and 637 are radio-quiet.

3 IDENTIFICATION OF PDLAS

We searched each of the 731 SDSS spectra for absorption features satisfying the following criteria:

- velocity $< 6000 \text{ km s}^{-1}$ blueward of the Ly α emission;
- saturated absorption trough (i.e. minimum consistent with zero residual flux);
- $N(\text{H I}) \geq 2.0 \times 10^{20} \text{ cm}^{-2}$ (corresponding to rest-frame equivalent width $\gtrsim 10\text{\AA}$).

The HI column densities, $N(\text{H I})$, of the candidates were measured by fitting theoretical Ly α absorption profiles to the spectra using the DIPSO package (Howarth et al. 2003), iterating in $N(\text{H I})$ and redshift until a good fit was found (usually after two iterations). We also searched for the strong metal absorption lines commonly associated with DLAs (Table 1) to help constrain the redshift. The search yielded 33 proximate DLAs (Table 2). Spectra of the PDLAs, as well as the $N(\text{H I})$ fits, are shown in Fig. 1.

A concern when working with moderate-to-low S:N spectra is the level of completeness in the absorber sample, either due to blending or underestimating the column densities near to the $2 \times 10^{20} \text{ cm}^{-2}$ limit. To quantify the completeness of our sample, we added simulated DLAs to real spectra of QSOs (blueward of Ly α) and attempted to recover them, adopting the same criteria as we used for the search for real DLAs. We simulated a range of column densities $N(\text{H I}) = 0.5, 1.0, 2.0$ and $3.0 \times 10^{20} \text{ cm}^{-2}$, and S:N per pixel = 3, 4, 5 and 6 (measured redward of Ly α). For each combination of S:N and $N(\text{H I})$ we created 40 simulated spectra, i.e. 640 spectra in all. The simulations and searches were made by different members of the team; the results are shown in Fig. 2. All of the simulated DLAs with $\text{S:N} \geq 5.0$ and $N(\text{H I}) \geq 2.0 \times 10^{20} \text{ cm}^{-2}$ were identified and recovered, indicating that our search for DLAs with $N(\text{H I}) \geq 2.0 \times 10^{20} \text{ cm}^{-2}$ and $\text{S:N} \geq 5$ is likely to be 100% complete. For $\text{S:N} = 4$, the completeness would be 93%.

Uncertainties in the $N(\text{H I})$ determinations come from both statistical and systematic (e.g. continuum fitting) errors. Prochaska, Herbert-Fort & Wolfe (2005) independently discovered, and measured the $N(\text{H I})$ of, 17 of the PDLAs in Table 2. 16 of these measurements of $N(\text{H I})$ agree with our values, within 0.2 dex. The column densities are not systematically over- or under-estimated by either group, so we consider 0.2 dex a realistic fiducial error which accounts for both statistical and systematic uncertainties.

Notes on individual PDLAs:

SDSS J014049.18–083942.5 This velocity-detached BAL QSO has a PDLA with strong O I and Si II absorption lines. These metal lines confirm the redshift derived from a good fit to the Voigt profile.

SDSS J080553.02+302937.3 The relatively high signal-to-noise ratio (S:N = 9.9 in the continuum redward of Ly α) produces an excellent profile fit, with little blending from neighbouring absorbers. Strong O I and C IV absorption defines the DLA redshift at just 200 km s^{-1} blueward of the Ly α emission line. With such a small relative velocity, this absorber could be associated with the QSO host galaxy. This is an interesting source to follow up with high resolution spectroscopy.

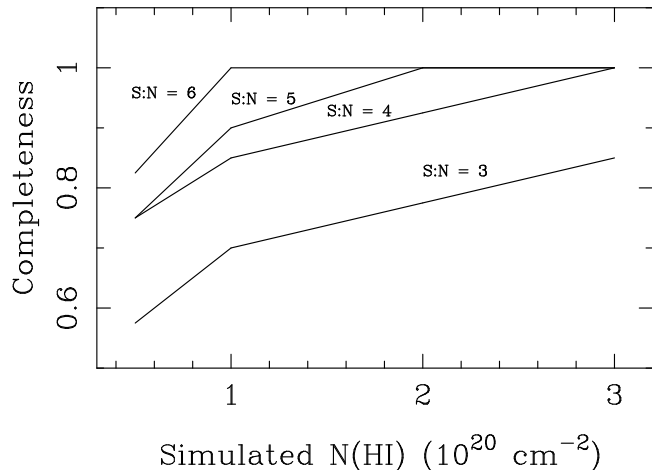


Figure 2. The fraction of simulated DLAs that were identified, as a function of the S:N on the quasar spectrum and the HI column density. For $\text{S:N} \geq 5$ and $N(\text{H I}) \geq 2.0 \times 10^{20} \text{ cm}^{-2}$, the completeness of the search is $\approx 100\%$.

SDSS J082638.59+515233.2 This relatively bright QSO ($i = 17.3$) possesses a PDLA with a well-defined fit, particularly in the trough, with $N(\text{H I}) = 5.5 \times 10^{20} \text{ cm}^{-2}$. Many strong metal lines are associated with the absorber; all those listed in Table 1 except the Al III line. A sub-DLA, $N(\text{H I}) = 1.3 \times 10^{20} \text{ cm}^{-2}$, is evident just to the red of the main DLA, velocity $\sim -850 \text{ km s}^{-1}$ (i.e. redward) of the QSO redshift. Three metal lines are detected in association with the sub-DLA: the blue component of the C IV doublet, and both components of the Si IV doublet. The Ly α emission line appears to be suppressed by these absorbers. A handful of multiple DLAs have been reported at intervening redshifts (e.g. Ellison & Lopez 2001; Lopez & Ellison 2003; Prochaska & Herbert-Fort 2004; Turnshek et al. 2004). Statistically, these are improbable events if the proximity of the systems is purely by chance, and they may trace large-scale structures (e.g. Ellison & Lopez 2001; Turnshek et al. 2004). The double DLA found towards this QSO has a separation $\Delta v \sim 2180 \text{ km s}^{-1}$.

SDSS J101122.59+470042.2 This RLQ (the brightest at radio wavelengths; $S_{1.4\text{GHz}} \sim 30 \text{ mJy}$) possesses a PDLA with heavy blending in the wings of the profile. However a good fit to the profile in the trough constrains the $N(\text{H I})$ and redshift, the latter of which is confirmed by a strong O I line.

SDSS J102619.09+613628.9 The DLA is detected in all the metal lines listed in Table 1, except the Al III line, which falls outside the range of the spectrum. The absorber is well-fitted by the Voigt profile in the trough and on the red wing, with narrow absorbers contaminating the fit to the blue wing.

SDSS J104820.93+503254.2 The redshift of this high $N(\text{H I})$ absorber cannot be accurately measured from the profile fit due to narrow blended absorbers, however 5 associated metal lines constrain the redshift in this high-S:N (12.0) spectrum.

SDSS J111224.18+004630.3 One of the highest column density PDLAs known ($N(\text{H I}) = 19 \times 10^{20} \text{ cm}^{-2}$), the redshift is well-constrained by the detection of O I and Al II lines. Many deep absorbers confuse the fit on the blue side of the trough, although the profile fits well on the red side and on both wings. However, this system exhibits the largest discrepancy with the $N(\text{H I})$ determined by Prochaska et al. (2005): $3.5 \times 10^{20} \text{ cm}^{-2}$. This is a good example of the significant errors that can arise when estimating $N(\text{H I})$ for DLAs which are heavily blended.

SDSS J134100.13+580724.2 A collection of very prominent metal lines (all those listed in Table 1) define the redshift of this PDLA. Despite contamination from deep neighbouring absorbers in the Ly α forest, the $N(\text{H I})$ is well-constrained by the fit in the trough and on the red wing.

SDSS J140029.01+411243.4 This PDLA not only possesses the largest column density reported in this paper (well fitted by a Voigt profile with $45 \times 10^{20} \text{ cm}^{-2}$), but is also just $\sim 250 \text{ km s}^{-1}$ blueward of the Ly α emission. The small velocity relative to the QSO suggests that the absorber may be associated with the host galaxy. Measurements of the absorber's metallicity may reveal its nature; many metal lines are seen in the SDSS spectrum, but the high equivalent widths indicate that they are all saturated and therefore not useful for abundance determinations.

SDSS J155248.01+560328.9 The estimated column density of $2.0 \times 10^{20} \text{ cm}^{-2}$ produces an acceptable fit, however a deep but narrow absorption line blends with the blue wing. Strong C IV absorption (1548 Å, 1550 Å) is detected at the redshift of this second feature, but no metal lines are detected in association with the PDLA.

SDSS J171800.20+621325.6 Two narrow but deep absorbers blend with the wings of this PDLA, but the redshift and column density are well-defined, by the fit in the trough and by four associated metal lines; O I, Si II, Fe II and Al II.

SDSS J210025.03-064146.0 This absorber has a high column density ($N(\text{H I}) = 9.0 \times 10^{20} \text{ cm}^{-2}$) and all the metal lines listed in Table 1 are detected.

4 THE DLA NUMBER DENSITY

The number density of DLAs per unit redshift $n(z)$ is obtained by dividing the number of DLAs found by the total redshift path sampled, Δz and is quoted for a given mean redshift:

$$\Delta z = \sum_{i=1}^N (z_{\text{max},i} - z_{\text{min},i})$$

where $z_{\text{max},i}$ here is the QSO systematic redshift $z_{\text{sys},i}$, $z_{\text{min},i}$ is the redshift corresponding to a given velocity limit, and the summation is over the N QSOs in the sample. For the samples of radio-quiet and radio-loud QSOs, $N = 637$ and 94 respectively. The values of Δv , $z_{\text{min},i}$ and $z_{\text{sys},i}$ are related by:

$$r = \frac{1 + z_{\text{sys},i}}{1 + z_{\text{min},i}} \quad (1)$$

$$\frac{\Delta v}{c} = \frac{r^2 - 1}{r^2 + 1} \quad (2)$$

Equation (1) can be rewritten:

$$z_{\text{sys},i} - z_{\text{min},i} = \left(1 - \frac{1}{r}\right) (1 + z_{\text{sys},i}) \quad (3)$$

We measure $n(z)$ for the velocity ranges (1) $\Delta v < 6000 \text{ km s}^{-1}$, and (2) $\Delta v < 3000 \text{ km s}^{-1}$ (which is the most frequently used velocity cut-off in DLA surveys). For $\Delta v < 6000 \text{ km s}^{-1}$ ($r = 1.0202$), equation 3 yields the total redshift intervals searched for the 637 radio-quiet and 94 radio-loud QSOs:

$$\Delta z_{\text{rq}} = \sum_{i=1}^{637} (z_{\text{sys},i} - z_{\text{min},i}) = 55.02$$

$$\Delta z_{\text{rl}} = \sum_{i=1}^{94} (z_{\text{sys},i} - z_{\text{min},i}) = 7.74$$

We discovered 29 radio-quiet QSOs with PDLAs so the number density for radio-quiet QSOs is:

$$n(z)_{\text{rq}} = \frac{29}{55.02} = 0.53_{-0.10}^{+0.12}$$

(using 1σ confidence limits given by the Poissonian small number statistics; Gehrels 1986) and the number density for the radio-loud QSOs (4 PDLAs discovered) is:

$$n(z)_{\text{rl}} = \frac{4}{7.74} = 0.52_{-0.25}^{+0.41}$$

Repeating the calculations for a search limit $v < 3000 \text{ km s}^{-1}$ ($r = 1.0101$), we find $\Delta z_{\text{rq}} = 27.64$, and $\Delta z_{\text{rl}} = 3.89$. We discovered 11 radio-quiet QSOs and 1 radio-loud QSO with PDLAs within 3000 km s^{-1} (see Table 2), so the implied $n(z)$ are $n(z)_{\text{rq}} = 0.40_{-0.12}^{+0.16}$ and $n(z)_{\text{rl}} = 0.26_{-0.21}^{+0.59}$ per unit redshift. We compare in Table 3 our measured values of $n(z)$ for PDLAs with those from previous surveys, and with those predicted for intervening DLAs by Storrie-Lombardi & Wolfe's (2000) empirical formula $n(z) = 0.055(1+z)^{1.11}$. The $n(z)$ of the complete DR3 sample of intervening DLAs is in good agreement with Storrie-Lombardi & Wolfe over the redshift range studied here (J. X. Prochaska, private communication).

As a check of our method of measuring $n(z)$, we searched for intervening DLAs (with any velocity) in 40 randomly-selected SDSS QSOs with a distribution of redshifts similar to that in Table 2. We found nine (row 7 of Table 3), with a distribution of column densities consistent with that in Fig. 3. The implied $n(z)$ is $0.22_{-0.07}^{+0.10}$, in good agreement with the value of 0.26 predicted by Storrie-Lombardi & Wolfe, for $\langle z_{\text{abs}} \rangle = 3.08$.

To compare the distribution of PDLA $N(\text{H I})$ column densities with that reported for intervening DLAs in the SDSS DR3 (from Prochaska et al. 2005), we applied a Kolmogorov-Smirnov (K-S) test. The K-S probability that the distributions of PDLA and intervening DLA $N(\text{H I})$ column densities differ is 93% (the maximum difference between the cumulative distributions is 0.23), slightly less than

Table 3. Number density of DLAs per unit redshift, $n(z)$, for different samples and velocity ranges

Sample	QSO Type	No. of QSOs	Δv limit (km s ⁻¹)	N_{PDLA}	Δz_v	$n(z)_{PDLA}$	$\langle z_{abs} \rangle$	N_{DLA} expected	overdensity
(1)	(2)	(3)	(4)	(5)	(6)	(7)	(8)	(9)	(10)
(1) SDSS	RQQ	637	6000	29	55.02	$0.53^{+0.12}_{-0.10}$	3.521	16.0	1.8
(2) SDSS	RQQ	637	3000	11	27.64	$0.40^{+0.16}_{-0.12}$	3.361	7.7	1.4
(3) SDSS	RLQ	94	6000	4	7.74	$0.52^{+0.41}_{-0.25}$	3.466	2.2	1.8
(4) SDSS+CORALS+FBQS	RLQ	190	3000	5	7.47	$0.67^{+0.45}_{-0.29}$	2.790	1.8	2.8
(5) SDSS	All	731	6000	33	62.76	$0.53^{+0.11}_{-0.09}$	3.515	18.2	1.8
(6) All Above Surveys	All	827	3000	16	35.11	$0.46^{+0.14}_{-0.11}$	3.182	9.5	1.7
(7) SDSS	RQQ	40	none	9	40.52	$0.22^{+0.10}_{-0.07}$	3.08	10.5	0.8

The columns give: (1) PDLA sample = SDSS (this paper), the CORALS Survey (Ellison et al. 2002), FBQS (FIRST Bright Quasar Survey, White et al. 2000); (2) QSO type, radio-quiet or radio-loud; (3) number of QSOs in the sample; (4) velocity limit; (5) number of DLAs found within given Δv ; (6) total redshift path Δz searched; (7) number density $n(z)$ and statistical error; (8) mean redshift of DLAs; (9) number of intervening DLAs predicted for a redshift path Δz_v , using the formula of Storrie-Lombardi & Wolfe (2000); (10) overdensity of PDLAs N_{PDLA} / N_{DLA} . The statistical significance of there being an overdensity is 3.0σ , 1.4σ , 1.4σ and 3.5σ in rows 1, 2, 3 and 5 respectively, as estimated from Monte Carlo simulations (see §4). Row (7) gives the result of our search for intervening DLAs in 40 SDSS spectra (a check of our search method).

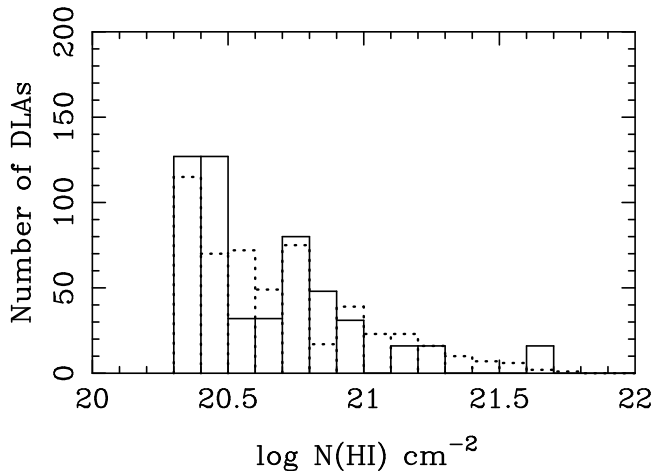


Figure 3. Distribution of $N(\text{H I})$ column densities of the PDLAs discovered here (solid line) compared with that of the intervening DLAs from SDSS DR3 (Prochaska et al. 2005; dashed line). The y-axis refers to the number of DLAs in the sample of Prochaska et al. (total 525). To facilitate comparison, our sample of PDLAs has been normalised such that it has the same total area under the histogram.

a 2σ result. However, K-S test results require at least a 95% probability before they are usually considered to provide evidence against the null hypothesis. It is therefore uncertain from Fig. 3 and the K-S test results whether the distributions differ in a systematic way. In §5.2 we return to the issue of $N(\text{H I})$ differences between PDLAs and DLAs.

A possible source of error in the measured $n(z)$ (which could also affect the K-S test) is the error in measuring $N(\text{H I})$, which is particularly critical near the $2 \times 10^{20} \text{ cm}^{-2}$ cut-off. If the number of $N(\text{H I})$ values (Fig. 3) rises as

$N(\text{H I})$ decreases, then measurement error could promote more $N(\text{H I})$ values above the limit of $2.0 \times 10^{20} \text{ cm}^{-2}$ than are pushed below it (a Malmquist bias; e.g. Rao & Turnshek 2000). Using the $N(\text{H I})$ column-density distribution given in Fig. 4 of Ellison et al. (2001), we estimate that the measured number of DLAs in the range $20.3 \leq \log N(\text{H I}) < 20.4$ will exceed the true value by only $\sim 3\%$, i.e. the error in $n(z)$ is negligible compared to statistical noise. For the 17 DLAs in common with the Prochaska et al. (2005) work, we see that not only are the column densities generally in good agreement (80% agree within ± 0.1 dex), but there is no systematic over- or under-estimate by either group. Measurement errors are therefore unlikely to dominate the K-S test.

Finally, we investigated the possibility that our measurements of $n(z)$ might depend on the redshift range used, because the Ly α forest is usually noisier in high-redshift QSOs, making it more difficult to fit profiles to candidate DLAs. We recalculated $n(z)$ for QSOs with $z_{\text{sys}} \leq 3.5$, removing from the sample the 16 highest redshift PDLAs with $\Delta z < 6000 \text{ km s}^{-1}$. The 17 remaining low-redshift PDLAs with $\Delta z < 6000 \text{ km s}^{-1}$ give $n(z) = 0.53^{+0.16}_{-0.13}$ (with redshift range $\Delta z_v = 32.14$), and the 6 low-redshift PDLAs with $\Delta z < 3000 \text{ km s}^{-1}$ yield $n(z) = 0.37^{+0.22}_{-0.15}$ ($\Delta z_v = 16.15$). These values of $n(z)$ are consistent with $n(z)$ measured using all the PDLAs, implying that the inclusion of high redshift systems does not significantly bias our result.

We find (Table 3) that the number densities of PDLAs $n(z)_{PDLA}$ exceed the expected values for intervening DLAs $n(z)_{DLA}$ given by Storrie-Lombardi & Wolfe (2000). To estimate the significance of these apparent overdensities we need to consider the errors associated with the expected number density for intervening systems, as well as the Poisson er-

Table 4. $n(z)_{DLA}$ from Storrie-Lombardi & Wolfe (2000) and 1σ confidence limits determined by us (see §4).

redshift range	Δz	N_{DLA}	$n(z)_{DLA}$
2.5 - 3.0	76.9	15	$0.20^{+0.06}_{-0.05}$
3.0 - 3.5	40.9	10	$0.24^{+0.11}_{-0.07}$
3.5 - 4.7	33.8	12	$0.36^{+0.13}_{-0.11}$

rors quoted for the PDLAs. For the intervening DLAs we determine the statistical error on $n(z)$ using Monte Carlo simulations of our QSO catalogue. We start by determining 1σ confidence limits (Gehrels 1986) associated with $n(z)_{DLA}$ as a function of redshift from Table 9 of Storrie-Lombardi & Wolfe (2000). The results are shown in Table 4. We then took 731 QSOs with a redshift distribution identical to our SDSS sample and allocated a number density $n(z)_{rand}$ drawn from a Gaussian distribution, $n(z)_{DLA} \pm \sigma$, for each QSO. Using Poisson statistics, the probability of finding m DLAs for a given QSO was calculated; $P(m) = e^{-N} N^m / m!$, where N is the expected number of DLAs for a given QSO; $N = N_{DLA} = n(z)_{rand} \Delta z_v$. In this way, we determined the number of intervening DLAs, N_{DLA} , expected at $\Delta v < 6000$ km s⁻¹.

We produced 10,000 realisations of the 731 QSO sample; in Fig. 4 we show a histogram of N_{DLA} corresponding to the 731 QSOs in row 5 of Table 3. The mean number of DLAs at $\Delta v < 6000$ km s⁻¹ in our simulations is $N_{DLA} = 18.2 \pm 4.2$, compared with the observed value of $N_{PDLA} = 33$, a difference of 3.5σ . From this we conclude that there is a statistically significant excess of DLAs at small velocity separations.

In fact, 33 or more PDLAs were found in only 0.05% of our simulations. The inferred significance of there being an overdensity of DLAs in each SDSS QSO sample is shown in the footnotes of Table 3. The redshifts of each QSO in the samples from the literature are unavailable and so the significance of the overdensity could not be calculated in these samples.

5 DISCUSSION

5.1 An Excess of PDLAs at $\Delta v < 6000$ km s⁻¹ and dependence on Radio-Loudness

We begin by considering the number density in the full 731 SDSS QSO sample used in this work to address the first question posed in the introduction: is the density of DLAs in the vicinity of QSOs significantly higher than that along the line of sight? From rows 5 and 6 of Table 3 we find a factor of ~ 2 overdensity of $n(z)_{PDLA}$ compared with intervening systems for velocities < 3000 and < 6000 km s⁻¹ (overdense at 3.5σ significance for $\Delta v < 6000$ km s⁻¹).

Dividing our sample between radio-loud and radio-quiet QSOs we can address the second question of the introduction: do the environments of RQQs differ from those of RLQs? For RQQs within $\Delta v < 6000$ km s⁻¹ (row 1 of Table 3), the measured $n(z)_{PDLA}$ exceeds $n(z)_{DLA}$ (or N_{PDLA} exceeds N_{DLA}) by a factor 1.8; an overdensity of DLAs at the 3.0σ level. For $\Delta v < 3000$ km s⁻¹ (row 2 of Table 3),

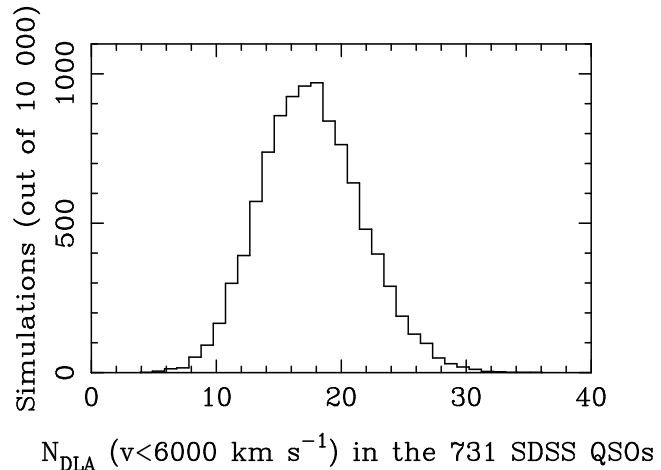


Figure 4. Distribution of numbers of PDLAs found in Monte Carlo simulations of samples of 731 QSOs with the same redshift distribution as the SDSS sample. PDLAs have been included with the $n(z)$ determined by Storrie-Lombardi & Wolfe (2000). Errors in $n(z)$ have been included based on the Storrie-Lombardi & Wolfe error bars drawn from a Gaussian distribution. The actual number of PDLAs found in the SDSS was 33; this number (or higher) occurred in 0.05% of Monte Carlo realisations.

an excess is also apparent, but only significant at the 1.4σ level. A similar excess of PDLAs is found for RLQs ($\Delta v < 6000$ km s⁻¹), but is significant at just the $\sim 1.4\sigma$ level, due to the small number of PDLAs in the sample (4 PDLAs; Table 3 row 3). We find just one PDLA within $\Delta v < 3000$ km s⁻¹ amongst the RLQs in our sample, but by combining our result with those from the CORALS (Ellison et al. 2002) and FBQS (White et al. 2000) samples of RLQ PDLAs, we raise this number to five (row 4 of Table 3), and find again that $n(z)$ exceeds the value for intervening absorbers, this time by a factor 2.8 (no error quoted on the FBQS sample).

We therefore confirm the excess of DLAs close to the redshift of RLQs seen by Ellison et al. (2002), but we find that a similar excess is present in the vicinity of RQQs with no significant difference between the two environments.

The excess of absorbers within 6000 km s⁻¹ of both RQQs and RLQs may be due to galaxies in the same cluster or supercluster as the QSO. Overdensities of galaxies associated with quasars have been noted by many authors (see §1). However, velocity distributions of galaxies within individual clusters at $z \sim 0$ are typically ~ 1000 km s⁻¹, so the apparent overdensities found here ($\Delta v < 6000$ km s⁻¹) imply structure on supercluster scales. Calculating the physical distance between QSOs and PDLAs is not straightforward, particularly if both are located in a large mass potential where peculiar velocities dominate. We can only calculate the line of sight separations under the assumption that the velocities are driven by the Hubble flow. In this case (which of course is not valid if the overdensities are linked to clustering) we find QSO-PDLA separations up to 70 comoving Mpc.

Many authors have reported galaxy clustering around QSOs on scales of a few comoving Mpc (e.g. Söchting, Clowes & Campusano 2004 and references therein) whilst QSOs themselves seem to cluster over similar distances (Croom et al. 2004; Porciani, Magliocchetti & Norberg

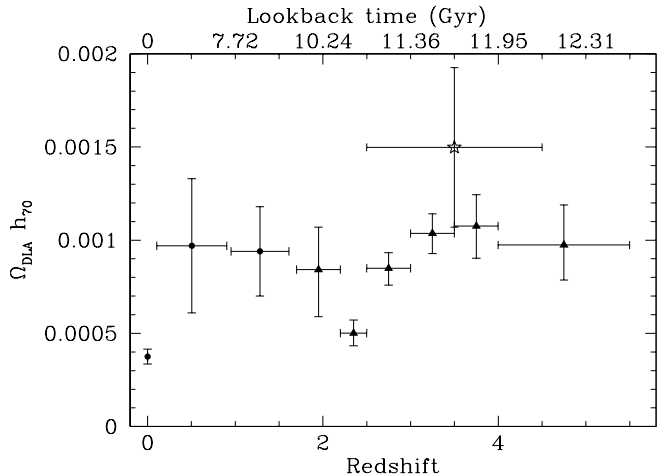


Figure 5. Mass density of neutral gas as a function of redshift. Intervening DLAs from the SDSS DR3 (Prochaska et al. 2005) are shown as filled triangles. Low redshift (Rao 2005) and $z = 0$ (Zwaan et al. 2005) data are shown with filled circles. The value determined for PDLAs (this work) in DR3 is shown with an open star.

2004). Even larger scale structures have been reported ranging from tens (Steidel et al. 1998; Söchtig, Clowes & Campusano 2002; Haines et al. 2003) to hundreds (Quashnock, Vanden Berk & York 1996; Loh, Quashnock & Stein 2001; Haines, Campusano & Clowes 2004) of comoving Mpc. Large scale structures of many Mpc are therefore pervasive from the lowest (e.g. Geller & Huchra 1989) to the highest ($z \sim 6$; Stiavelli et al. 2005) redshifts observed. An excess of PDLAs, if the overdensities can be linked to clustering, is not surprising given the considerable body of work that supports galaxy clustering over such large volumes. The extent of the overdensity, in the range $\sim 40\%$ to a factor of two, is also consistent with what has been seen in galaxy surveys (e.g. Sanchez & Gonzalez-Serrano 1999; Williger et al. 2002; Haines et al. 2004; Overzier et al. 2005). Our observations of PDLAs could therefore confirm the scale and extent of galaxy excesses that have been previously mapped in 2 dimensions.

5.2 The Neutral Gas Content of PDLAs

In addition to the number density of PDLAs, we can also calculate the mass density of neutral gas as a fraction of the closure density, Ω_{DLA} :

$$\Omega_{DLA} = \frac{H_0 \mu m_H \sum_i N_i(\text{H I})}{c \rho_{crit} \Delta X} \quad (4)$$

where μ is the mean molecular weight ($= 1.3$) and m_H is the mass of a hydrogen atom. Note that only neutral gas contributes to this quantity, so gas that has been ionised, e.g. due to the proximity of the QSO is not included in the sum. For our adopted cosmology X and z are related by the equation

$$X(z) = \int_0^z (1+z)^2 [(1+z)^2 (1+z\Omega_M) - z(2+z)\Omega_\Lambda]^{-1/2} dz \quad (5)$$

Table 5. $n(z)_{PDLA}$ derived for different velocity ranges, to check the effect of systematic errors in velocity.

Δv (km s $^{-1}$)	N_{PDLA}	$n(z)_{PDLA}$
0 - 3000	12	$0.38^{+0.14}_{-0.11}$
100 - 3100	12	$0.38^{+0.14}_{-0.11}$
200 - 3200	16	$0.51^{+0.16}_{-0.13}$
500 - 3500	17	$0.54^{+0.17}_{-0.13}$

The errors associated with $n(z)_{PDLA}$ are 1σ confidence limits (Gehrels 1986).

ΔX is therefore calculated analogously to δz by summing over the 731 QSOs in our sample. We determined $\log \Omega_{DLA} h_{70} = -2.82^{+0.110}_{-0.146}$, with errors calculated as in Storrie-Lombardi, Irwin & McMahon (1996). In Fig. 5 we compare the values determined for Ω_{DLA} in the intervening DLA population in the DR3 (Prochaska et al. 2005) and at low redshift (Rao 2005; Zwaan et al. 2005) with the value determined for PDLAs. The PDLA value is $\sim 50\%$ larger than for the intervening systems, but also is consistent within the large error bars with the DLA value. If the higher Ω_{DLA} for PDLAs is confirmed, this may simply reflect the excess of the number density, $n(z)$, if the distribution of column densities of neutral hydrogen are similar. However, since Ω_{DLA} is dominated by the rare high $N(\text{H I})$ systems, the gas mass density is very sensitive to small sample sizes. We have 33 PDLAs in our sample, whereas each of the $z > 2$ SDSS bins typically contains 100 – 200 DLAs. If we exclude our highest column density system from the calculation, Ω_{DLA} for PDLAs is in excellent agreement with the intervening systems. Similarly, if we include a further high- $N(\text{H I})$ system, Ω_{DLA} for PDLAs is \sim twice that of the intervening DLAs, a result consistent with the observed excess of proximate DLAs and similar sample average $N(\text{H I})$.

5.3 The Systemic Redshift of QSOs and PDLA Velocity Distribution

Our definition of PDLAs is based on relatively small velocity offsets, which in turn are dependent upon accurate systemic redshifts. It has been known for decades that there are systemic shifts between the high ionisation broad emission lines (e.g. Gaskell 1982; with recent reviews by Richards et al. 2002 and Vanden Berk et al. 2001). The systemic redshifts of QSOs in SDSS are determined from a cross-correlation of the spectrum with the composite of Vanden Berk et al. (2001), which itself is constructed by assuming the forbidden [O III] line (5007Å) is representative of the true systemic redshift. This technique minimises the systemic offset that may occur when measuring the redshift of a QSO from the Ly α emission line if the line is blended by a PDLA. However, the scatter in blue/redshifts of Ly α (in particular, since it is the strongest emission line covered in our redshift range) relative to [O III] will contribute an uncertainty in the redshift. This scatter between $z_{\text{Ly}\alpha}$ and $z_{[\text{O III}]}$ is relatively small however; from Vanden Berk et al. (2001) $\Delta v = 143 \pm 91$ km s $^{-1}$.

In order to assess the impact of uncertainties in z_{sys} we have calculated $n(z)_{PDLA}$ in different velocity bins where the lower limit (always assumed to be zero in our original

calculations) is offset by 100, 200 and 500 km s⁻¹ (Δv is held constant). The results are presented in Table 5. Although there is some variation in the different velocity bins, the number densities are consistent with each other within the Poisson errors (again, calculated from Gehrels 1986). Therefore, although an individual QSO may have an error of several hundred km s⁻¹ in its quoted systemic redshift, this is unlikely to reproduce an excess of PDLAs within several thousand km s⁻¹.

Fig. 6 shows a histogram of the distribution of PDLA velocities relative to z_{sys} . We have binned the histogram relatively coarsely (Δ 1000 km s⁻¹) due to the errors in redshift discussed above and also the modest sample size. The apparent peak of the distribution lies at \sim 3500 km s⁻¹, and the intervening DLA number density is recovered by $\Delta z \sim$ 6000 km s⁻¹. However, the position of the peak is not highly significant, and the distribution suffers from low number statistics. Despite the low number statistics it is interesting to note that Williger et al. (2002) also found *transverse* overdensities between MgII absorbers and QSOs on scales 3000–4500 km s⁻¹ (albeit in one velocity direction only).

Prochaska et al. (2005) published a statistical sample of SDSS DLAs in the DR3 which excludes proximate systems. However, this cut was done *a posteriori* and PDLAs were identified in their ‘full’ DLA list. Although the selection criteria of the Prochaska et al. sample are somewhat different to ours (e.g. based on colour selection, S:N redshift range and FIRST coverage), we can calculate relative numbers of PDLAs to intervening DLAs from their full sample (Prochaska, 2005, private communication) which is continuous in velocity distribution. The overdensity of PDLAs found by us is replicated in the Prochaska et al. sample which contains 50 DLAs at $\Delta v < 3000$ km s⁻¹², a factor of \sim 10 more than found in similar velocity width bins at $v \gg 6000$ km/s. The Prochaska et al. sample also confirms that by $v=6000$ km s⁻¹ the number density has fallen to the background level.

In theory, the distribution of galaxy velocities in the field of a given QSO can provide information of the environment, such as the mass potential. Here, however, the interpretation of velocity distribution is not straightforward. Each PDLA is likely to inhabit a different environment and the QSOs possess a range of properties such as luminosity and radio-loudness. With a large number of absorbers, distinct populations may be discerned. For example, Weymann et al. (1979) produced a histogram like Fig. 6, for a large number of C IV absorbers and divided the populations into ‘intervening’ and ‘ejected’ components. Larger samples of PDLAs may be used to distinguish the velocity distributions of absorbers associated with galaxy overdensities near QSOs. With the final releases of SDSS data to follow, a further 2400 degrees² of spectroscopic sky coverage (and hence many PDLAs) is expected to be available. It will then be possible to measure the excesses we find more accurately, reducing the errors in $n(z)$. It may also be possible to measure $n(z)$ as a function of velocity from the quasar. With the

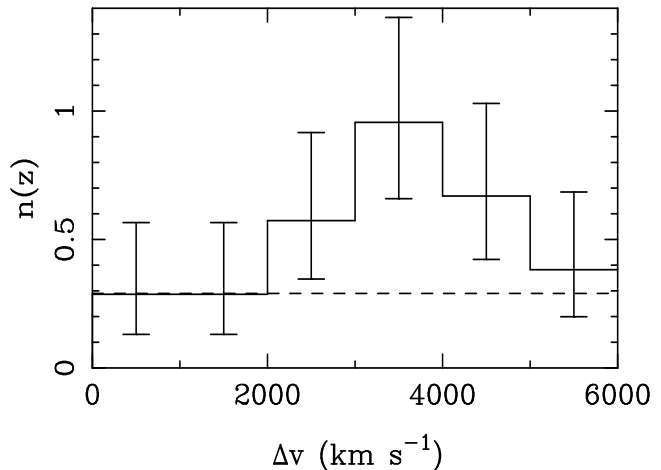


Figure 6. $n(z)_{DLA}$ found in SDSS as a function of Δv . The bins are 1000 km s⁻¹ wide. The dashed line indicates the expected number density for intervening DLAs $n(z)_{DLA}$.

current statistics we can only note that by $v \sim 6000$ km s⁻¹ the number density is close to that of the intervening DLAs.

Finally, we note that the clustering of DLAs around QSOs could be independently checked by observing QSO pairs with slightly different redshifts, but modest impact parameters (e.g. Hennawi et al. 2005). If DLAs preferentially occur near QSOs, we would expect to see the same overdensity of DLAs at approximately the redshift of the nearer of the pair imprinted on the spectrum of the more distant QSO.

6 CONCLUSIONS

We have searched the spectra of 731 SDSS DR3 $2.5 < z_{sys} < 4.5$ QSOs for DLAs ($N(\text{H I}) > 2 \times 10^{20}$ cm⁻²) and found 33 within $\Delta v < 6000$ km s⁻¹ (and 12 within $\Delta v < 3000$ km s⁻¹). Our search increases the number of PDLAs reported in the literature within $\Delta v < 3000$ km s⁻¹ (the conventional definition of $z_{abs} \sim z_{sys}$ DLAs) from 5 to 16.

The number density of DLAs within $\Delta v < 6000$ km s⁻¹ of the redshift of the QSOs is approximately double that observed for samples of intervening DLAs (a) found in the same sample, the SDSS (Prochaska et al. 2005) and (b) for the relation derived by Storrie-Lombardi & Wolfe (2000). The excess is significant at the 3.5 σ level. There is no significant difference between the number density of PDLAs towards RLQs and RQQs. A similar excess of PDLAs is found within $\Delta v < 3000$ km s⁻¹ of QSOs; $n(z)_{PDLA} / n(z)_{DLA} = 1.7$ for all RQQs and RLQs combined. We speculate that the overdensities of DLAs in the vicinity of QSOs may trace galaxies in the same clusters or superclusters as the QSOs. The similar excesses around radio-quiet and radio-loud quasars are consistent with their inhabiting similar environments, as suggested by recent observations (e.g. Finn, Impey & Hooper 2001; Wold et al. 2001). This emphasises the importance of imposing a velocity cut when studying intervening DLAs, not only to avoid intrinsic AGN absorption, and any proximity effect, but also to avoid objects in the cluster or supercluster hosting the QSO. Moreover, we recommend

² This number is larger than the number of PDLAs in our sample because of the less stringent selection conditions imposed by Prochaska et al. (2005) on their parent QSO sample.

that, based on Fig. 6, $\Delta v \sim 6000 \text{ km s}^{-1}$ is a suitable velocity cut.

A number of PDLAs in the DR3 exhibit strong metal lines, despite the moderate resolution and S:N ratios of the spectra. With high-resolution spectroscopy, it should be possible to determine whether the metallicities of PDLAs are enhanced compared with intervening DLAs, as may be expected if they are associated with the QSO environment. For example, Ellison & Lopez (2001) and Lopez & Ellison (2003) found unusual relative abundances in a pair and a triplet of DLAs whose velocity separations were $< 10\,000 \text{ km s}^{-1}$. Many QSOs in the SDSS are bright enough to follow-up with an echelle spectrograph on an 8-m telescope, such as UVES on the VLT. Investigating the abundances of PDLAs will be an interesting, and so far unexplored, extension of this work.

Acknowledgements. We are grateful to Jason X. Prochaska for providing the statistics for the intervening DLAs discovered in Data Release 3 prior to publication, and to Patrick B. Hall for valuable advice on the SDSS database. Funding for the creation and distribution of the SDSS Archive has been provided by the Alfred P. Sloan Foundation, the Participating Institutions, the National Aeronautics and Space Administration, the National Science Foundation, the U.S. Department of Energy, the Japanese Monbukagakusho, and the Max Planck Society. The SDSS Web site is <http://www.sdss.org/>.

The SDSS is managed by the Astrophysical Research Consortium (ARC) for the Participating Institutions. The Participating Institutions are The University of Chicago, Fermilab, the Institute for Advanced Study, the Japan Participation Group, The Johns Hopkins University, the Korean Scientist Group, Los Alamos National Laboratory, the Max-Planck-Institute for Astronomy (MPIA), the Max-Planck-Institute for Astrophysics (MPA), New Mexico State University, University of Pittsburgh, University of Portsmouth, Princeton University, the United States Naval Observatory, and the University of Washington.

REFERENCES

- Abazajian K., et al. 2005, AJ, 129, 1755
 Adelberger K., Steidel C. C., Kollmeier J. A., Reddy N. A., 2005, ApJ, accepted, astro-ph/0509229
 Bahcall J. N., Schmidt M., Gunn J. E., 1969, ApJ, 157, L77
 Bajtlik S., Duncan R. C., Ostriker J. P., 1988, ApJ, 327, 570
 Barlow T. A., Sargent W. L. W., 1997, AJ, 113, 136
 Becker R.H., White R. L., Helfand D. J., 1995, ApJ, 450, 559
 Clements D., 2000, MNRAS, 312, 61
 Croom S. M. et al., 2004, ASPC, 311, 457
 D’Odorico V., Cristiani S., Romano D., Granato G. L., Danese L., 2004, MSAIS, 5, 227
 Ellingson E., Green R. F., Yee H. K. C., 1991, ApJ, 378, 476
 Ellison S. L., Yan L., Hook I., Pettini M., Wall J, Shaver P., 2001, A&A, 379, 393
 Ellison S. L., Yan L., Hook I., Pettini M., Wall J, Shaver P., 2002, A&A, 383, 91
 Ellison S. L., Lopez S., 2001, A&A, 380, 117
 Finn R., Impey C., Hooper E., 2001, ApJ, 557, 578
 Gaskell C. M., 1982, ApJ, 263, 79
 Geller M. J., Huchra J. P., 1989, Science, 246, 897
 Gehrels N., 1986, ApJ, 303, 336
 Haines C. P., Campusano L. E., Clowes R. G., 2004, A&A, 421, 157
 Haines C. P., Clowes R. G., Campusano L. E., Williger G. M., Graham M. J., 2003, IAUS, 216, 73
 Hall P., Green R., 1998, ApJ, 507, 558
 Hall P., Green R., Cohen M., 1998, ApJS, 119, 1
 Hennawi J., Strauss M. A., Oguri M., Inada N., Richards G. T., Pindor B., Schneider D. P. et al, 2005, AJ, submitted, astro-ph/0504535
 Howarth I. D., Murray J., Mills D., Berry D. S., 2003, Starlink User Note 50
 Loh J-M., Quashnock J. M., Stein M. L., 2001, ApJ, 560, 606
 Lopez S., Ellison S. L., 2003, A&A, 403, 573
 Lu L., Sargent W. L. W., Barlow T. A., Churchill C. W., Vogt S. S., 1996, ApJS, 107, 475
 Lu L., Wolfe A. M., Turnshek D. A., 1991, ApJ, 367, 19
 McLure R.J., Dunlop J. S., 2001, MNRAS, 321, 515
 Meyer D. M., Welty D. E., York D. G., 1989, ApJ, 343, L37
 Møller P., Warren S. J., 1993, A&A, 270, 43
 Møller P., Warren S. J., Fynbo J. U., 1998, A&A, 330, 19
 Overzier R. A., 2005, ApJ, accepted, astro-ph/0509308
 Péroux C., Storrie-Lombardi L. J., McMahon R. G., Irwin M., Hook I. M. 2001, AJ, 121, 1799
 Petitjean P., Rauch M., Carswell R. F., 1994, A&A, 291, 29
 Pettini M., 2004, in “Cosmochemistry. The melting pot of the elements.” (XIII Canary Islands Winter School of Astrophysics, Puerto de la Cruz, Tenerife, Spain, 2001, edited by C. Esteban, R. J. Garcí López, A. Herrero, F. Sánchez, Cambridge University Press) p.257
 Pettini M., Hunstead R. W., King D. L., Smith L. J., 1995, in “QSO Absorption Lines” (Proceedings of the ESO Workshop Held at Garching, Germany, 1994, edited by Georges Meylan, Springer-Verlag Berlin Heidelberg New York) ESO Astrophysics Symposia, 1995., p.55
 Porciani C., Magliocchetti M., Norberg P., 2004, MNRAS, 355, 1010
 Prochaska J. X., Herbert-Fort S., 2004, PASP, 116, 622
 Prochaska J. X., Herbert-Fort S., Wolfe A. M., 2005, ApJ, accepted, astro-ph/0508361
 Rao S. M., Turnshek D. A., 2000, ApJS, 130, 1
 Rao S. M., 2005, Proceedings IAU Colloquium 199, ‘Probing Galaxies through Quasar Absorption Lines’, Williams, Shu, & Menard, eds
 Richards G. T., et al., 2002, AJ, 124, 1
 Quashnock J. M., Vanden Berk D. E., York D. G., 1996, ApJ, 472, L69
 Sanchez S., Gonzalez-Serrano J., 1999, A&A, 352, 383
 Sanchez S., Gonzalez-Serrano J., 2002, A&A, 396, 773
 Söchting I. K., Clowes R. G., Campusano L. E., 2002, MNRAS, 331, 569
 Söchting I. K., Clowes R. G., Campusano L. E., 2004, MNRAS, 347, 1241
 Steidel C. C., Adelberger K. L., Dickinson M., Giavalisco M., Pettini M., Kellogg M., 1998, ApJ, 492, 428
 Stiavelli M. et al., 2005, ApJ, 622, L1
 Stocke J. T., Morris S. L., Weymann R. J., Foltz C. B., 1992, ApJ, 396, 487
 Storrie-Lombardi L., Irwin M., McMahon R. G., 1996, MNRAS, 282, 1330
 Storrie-Lombardi L., Wolfe A. M. 2000, ApJ, 543, 552
 Turnshek D. A., Rao S. M., Nestor D. B., Vanden Berk D., Belfort-Mihalay M., Monier E. M., 2004, ApJ, 609, L53
 Vanden Berk D. E. et al., 2001, AJ, 122, 549
 Weymann R. J., Williams R. E., Peterson B. M., Turnshek D. A., 1979, ApJ, 234, 33
 White R. et al., 2000, ApJS, 126, 133
 Williger G. M., Campusano L. E., Clowes R. G., Graham M. J., 2002, ApJ, 578, 708

- Wold M., Lacy M., Lilje P., Serjeant S., 2001, MNRAS, 323, 231
Wolfe A. M., Gawiser E., Prochaska J. X., 2005, ARA&A, 43, 861
Yamada T., Tanaka I., Aragon-Salamanca A., Kodama T., Ohta
K., Arimoto N., 1997, ApJ, 487, 125
Yee H., Green R., 1987, AJ, 94, 618
Zwaan M. A., Meyer M. J., Staveley-Smith L., Webster R. L.,
2005, MNRAS, 359, 30